5th Australasian Congress on Applied Mechanics, ACAM 2007
10-12 December 2007, Brisbane, Australia

Numerical Simulation of Dental Resurfacing of a Feldspar Porcelain with Coarse Diamond Burs

Xiao-Fei Song[1], Ling Yin[2], Yi-Gang Han[1], Hui Wang[3], Jia Li[1]

[1]*School of Mechanical Engineering, Tianjin University, Tianjin 300072, China*
[2]*Department of Engineering, Australian National University, Canberra ACT 0200, Australia*
[3]*Analysis & Measurement Center, Tianjin University, Tianjin 300072, China*

Abstract: Dental bioceramics are more and more attractive to both dentists and patients due to their unique biocompatibility and esthetics; they can be fabricated efficiently using chair-side CAD/CAM dental systems. However, the failure rate of ceramic prostheses is noticeable high. The major clinical failure mode lies in surface and subsurface damage in the ceramic prostheses due to their inherent brittleness. In clinical practice, ceramic prostheses are intraorally adjusted and resurfaced using dental handpieces/burs for marginal and occlusal fit. The clinical adjustments using abrasive burs produce surface and subsurface damage in prostheses. This paper will address this issue via numerical simulation. Finite element analysis was utilised to model the dental resurfacing of a feldspar porcelain with coarse diamond burs and to predict the degrees of subsurface damage of the porcelain prostheses.

Keywords: Dental ceramics, Dental resurfacing, Diamond burs, FEA, Subsurface damage.

1 Introduction

Dental bioceramics are increasingly attractive due to their superior biocompatibility, esthetics and inertness [1]. These materials are able to be machined quickly to generate ceramic prostheses using dental chair-side computer-aided design/computer-aided manufacture (CAD/CAM) systems [2]. However, ceramics are brittle and subject to premature failure, especially in long-term cyclic loading and moist environments [3]. The reported clinical failure rate, approximately 3% per year for all-ceramic crowns, is unacceptably high relative to metal-core crowns [3,4]. Furthermore, analyses of clinically failed crowns have proven that catastrophic fracture had, in fact, always originated from surface and subsurface damage in ceramic prostheses [5].

In dentistry, ceramic prostheses are intraorally resurfaced and adjusted using dental high-speed handpieces and diamond burs for accurate marginal and occlusal fit. These dental machining processes induce surface and subsurface damage and contribute to clinical failure in ceramic prostheses [6]. Therefore, evaluation of dental resurfacing-dependent damage is particularly required in restorative dentistry. Studies were conducted on characterization of *in vitro* dental resurfacing of ceramic prostheses using dental handpieces and diamond burs [7,8]. Extensive chipping damage was found in ceramic prosthetic materials [7,8], especially in feldspar porcelains when using coarse diamond burs [7]. However, little attention was paid to the relations between subsurface damage in ceramic prostheses and dental operational parameters applied in intraoral dental resurfacing.

Finite element analysis (FEA) was successfully applied for prediction of subsurface damage depths in ceramic and glass machining using diamond tools [9–12]. The machining-induced depths of subsurface damage in ceramics were associated with the machining parameters [9–12]. In spite of its considerable applications in engineering, FEA of dental resurfacing processes is little reported.

In this paper, we report on FEA modelling of dental resurfacing of a feldspar porcelain with a coarse diamond bur for prediction of subsurface stress distributions and damage degrees. A two-dimensional FEA was conducted with dental operational parameters and material properties as input variables. The maximum principal stress fields and the depths of subsurface damage were estimated as functions of the dental operational parameters.

2 *In Vitro* Dental Resurfacing

In vitro computer-assisted dental resurfacing operations were conducted using a novel experimental apparatus [13]. During the *in vitro* resurfacing, the computer-assisted apparatus enabled a dental handpiece to realize precise feed and down feed movements. Figure 1 schematically shows the dental handpiece-bur-prosthesis movements during resurfacing of a ceramic prosthesis with clinical operational parameters.

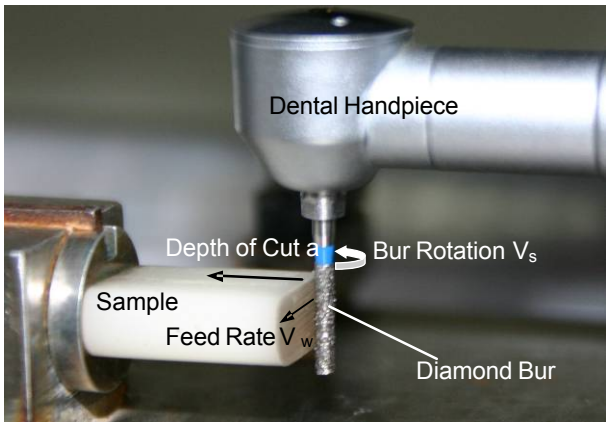

Figure 1. Dental handpiece-bur-sample movements.

Samples with dimensions 15×12×5 mm^3 were Vita Mark II (Vita Zahnfabrik, Bad Säckingen, Germany), which is a feldspar porcelain. The mechanical properties of the material are: Vickers hardness H = 6.2 GPa, Young's modulus E = 68 GPa, fracture toughness K_{IC} = 0.9 MPa.$m^{1/2}$, strength s = 100 MPa, and Poison's ration v = 0.2 [14,15].

A new nickel-coated, 106–125 μm grit diamond bur of diameter of 1.4 mm (SF-21, ISO 110523014, Mani, Japan) was used. The bur was aligned parallel to the 12×5 mm^2 surface of the prosthesis. During resurfacing, the dental bur, driven by applied pressure of 0.2 MPa at a free-running speed v_s of 318 krpm, was moved along the prosthetic surface at a depth of cut a and a feed rate v_w as shown in Figure 1. Water was sprayed onto the bur-prosthesis contact zone at a flow rate of 30 ml/min for cooling and cleaning of the resurfacing zone. The *in vitro* dental resurfacing operations were conducted where the depths of cut were in the range 10–50 μm, and feed rates of 15–60 mm/min. The actual bur speed during resurfacing was measured using a force sensor and a high-speed data acquisition system [13].

3 FEA Modelling

In dental resurfacing, the dental bur was manipulated to traverse the prosthetic surface for removal of a layer of material. Meanwhile, stress fields in the prosthesis are generated due to the interactions between the prosthetic material and the diamond grits. When these stresses exceed a threshold value, e.g., the ultimate strength of the material, it is likely that the subsurface damage zone will be produced in the prosthesis.

In this investigation, FEA was applied to model the dental resurfacing of a feldspar porcelain using commercial software, ANSYS 8.0 (ANSYS Incorporated, USA). The dental resurfacing process was treated as a static problem for simplification, since the focus of this study was subsurface stresses and the damage zone formed under bur-prosthesis contact loads. The porcelain material was assumed to be isotropic and homogeneous. The stresses and deformation produced were assumed to be within plane-strain conditions since the load and strain along the width of cut were nearly invariable during resurfacing. Thus, a two-dimensional plane-strain finite element model was established with dental operational parameters and material properties as input variables.

For the FEA geometric model, the dimensions were selected according to Saint-Venant's theory that stresses far from the point of load application must diminish [16]. The horizontal dimension was fixed at 0.8 mm, much larger than any depths of cut in the current study. The vertical dimension was 3 times the bur-prosthesis contact arc length, which is a function of depth of cut and diameter of bur. The loads with a set of displacement vectors were applied along the bur-prosthesis contact curve [11]. The magnitude of the imposed displacement vector equalled to the local chip thickness. As a single grit on the rotating bur moved along the contact curve, the local chip thickness increased gradually from zero at the grit entering point of the contact zone to the maximum undeformed chip thickness h_{max} at the grit exit point. The maximum undeformed chip thickness, i.e., the grit depth of cut, which can be expressed as [17]:

$$h_{max}=(3/C\tan\theta)^{1/2}(V_w/V_s)^{1/2}(a/d_s)^{1/4} \quad (1)$$

where C is the active cutting points per unit area, q is the semi-included angle for the undeformed chip cross-section, V_w is the feed rate, V_s is the bur speed, a is the depth of cut, and d_s is the bur diameter. For the bur grit size used in this study, C is taken as 20 and q as 60° [17,18]. The directions of the displacement vectors were assumed to vary gradually from the grit entering point to the grit exit point. At the grit entering point, the direction of the displacement vector was vertical to the feed rate direction; at the grit exit point, the direction was parallel to the feed rate.

Based on this FEA modelling, all stress components can be obtained. In particular, the maximum principal stress σ_t was of major interest. To quantitatively evaluate the resurfacing-induced subsurface damage, the maximum normal stress criterion associated with the failure of brittle material was applied. According to this criterion, it is assumed that subsurface damage initiates when the maximum principal stress σ_t exceeds the threshold value, i.e., the ultimate tensile strength σ of 100 MPa of the porcelain material. Thus, the depths of the resurfacing-induced subsurface damage were predicted in the porcelain under different dental operational conditions. A two-way factorial analysis of variance (ANOVA) at a 5% significant level was applied to examine the effects of the feed rate and depth of cut on the FEA-predicted maximum principal stress and subsurface damage depth.

4 Results

Figure 2(a) shows the maximum principal stress distribution under the bur-prosthesis contact zone at

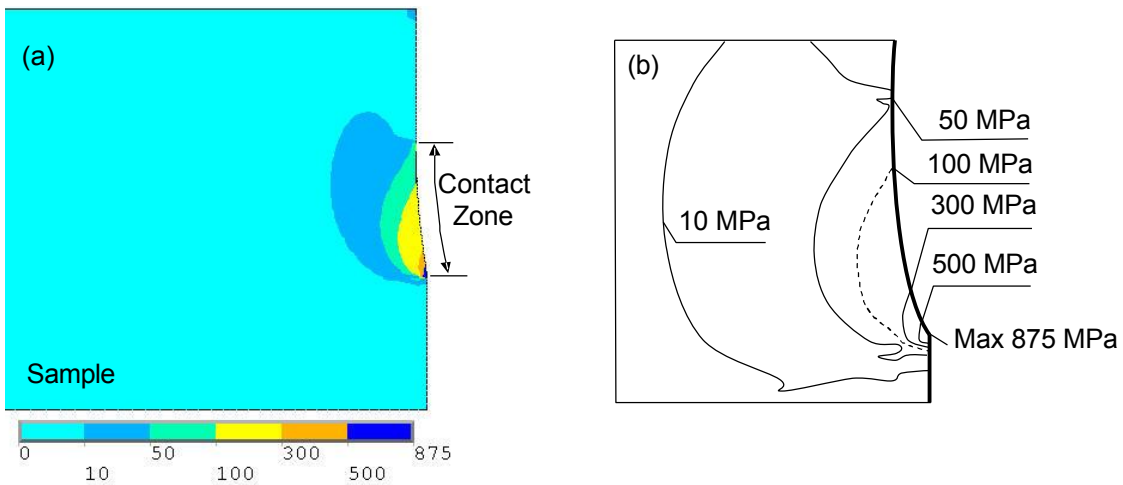

Figure 2. (a) Maximum principal stress distribution, and (b) detailed plot of stress distribution at the bur-prosthesis contact zone at a depth of cut of 10 μm and feed rate of 15 mm/min.

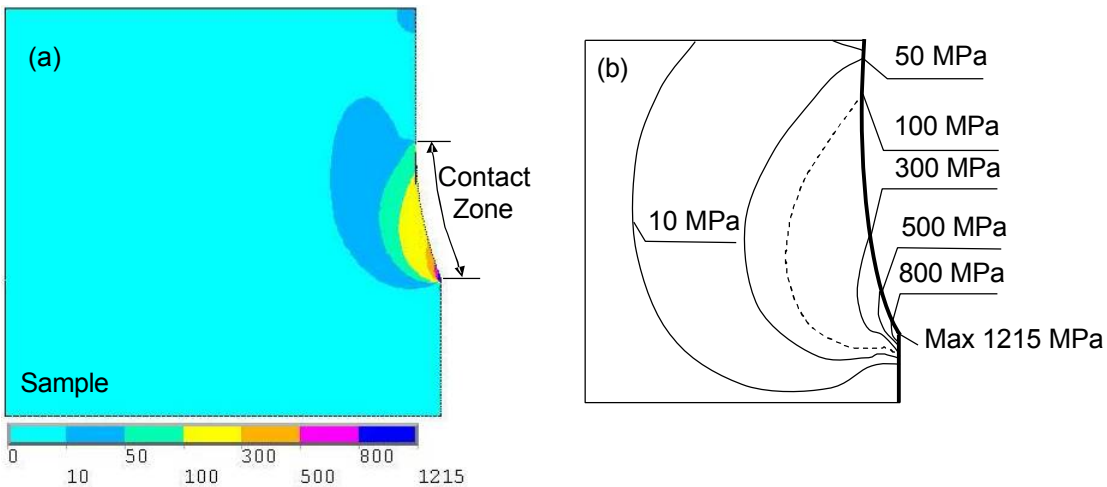

Figure 3. (a) Maximum principal stress distribution, and (b) detailed plot of stress distribution at the bur-prosthesis contact zone at a depth of cut of 50 μm and feed rate of 60 mm/min.

the depth of cut of 10 μm and the feed rate of 15 mm/min. It demonstrates that the maximum principal stresses were principally concentrated under the bur-prosthesis contact zone. The stress values decreased rapidly when increasing the distance to the contact surface. Figure 2(b) shows the detailed stress region near the contact zone. It reveals that the stress values significantly increased when approaching the diamond bur/grit exit point. The maximum principal stress reached the highest value of 875 MPa at the bur/grit exit point.

Figure 3(a) shows the maximum principal stress distribution under the bur-prosthesis contact zone at the depth of cut of 50 μm and the feed rate of 60 mm/min. Similar to the distribution trend in Figure 2(a), the maximum principal stresses were located under the bur-prosthesis contact zone and reduced quickly when increasing the distance to the contact surface. In comparison with the stress field shown in Figure 2, the maximum principal stresses at the deeper depth of cut and the higher feed rate were larger in magnitude and in distribution area. The detailed local stress field near the contact zone is shown in Figure 3(b). The maximum principal stress value of 1215 MPa occurred at the bur/grit exit point. For selected operational conditions in this investigation, it is also found that all the maximum principal stress values were concentrated at the bur/grit exits, in the range 601 MPa to 1755 MPa.

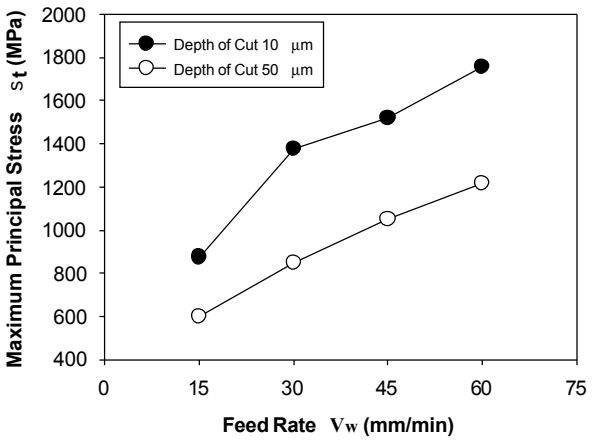

Figure 4. Maximum principal stress versus feed rate.

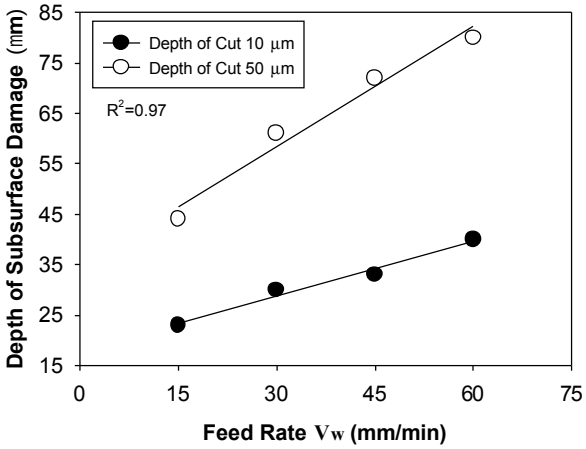

Figure 5. FEA-predicted depth of subsurface damage versus feed rate.

The maximum principal stress σ_t as a function of feed rate V_w for the depths of cut of 10 μm and 50 μm is plotted in Figure 4.The results show that maximum principal stress increased with the feed rate at each of the depth of cut. The increase in feed rate from 15 mm/min to 60 mm/min resulted in the doubling of the increase in maximum principal stress for both the depths of cut. Also, at any feed rate, the maximum principal stress values for the depth of cut of 10 μm were larger than those for the depth of cut of 50 μm. This indicates that at the smaller depth of cut, the maximum principal stress values were larger.

The FEA-predicted subsurface damage depth as a function of feed rate V_w for the depths of cut of 10 μm and 50 μm is plotted in Figure 5. It shows that subsurface damage depths for both the depths of cut increased linearly with the feed rate, with a coefficient of determination R^2 = 0.97. When increasing the feed rate from 15 mm/min to 60 mm/min, subsurface damage depths for the depths of cut of 10 μm and 50 μm increased by 74% and 82%, from 23 μm to 40 μm and from 44 μm to 80 μm, respectively. It is also found that subsurface damage depths for the depth of cut of 50 μm at any feed rate were approximately twice those for the depth of cut of 10 μm.

5 Discussion

We presented FEA modelling of dental resurfacing of a feldspar porcelain with a coarse diamond bur. In this model, stress distributions and subsurface damage degrees induced by dental resurfacing were the focus. For simplification, dynamic and thermal effects were not considered. The FEA results show that the trends for the maximum principal stress distributions under different operational conditions were similar. The maximum principal stresses were distributed near the bur-prosthesis contact zone

with a rapid decrease with the distance to the resurfaced surface. The maximum principal stress values were found almost at the bur/grit exits in spite of the differences in magnitude. This finding is in agreement with the results of FEA modelling of diamond wheel plunge grinding of silicon nitride [11]. A previous study found experimentally extensive edge chipping damage occurring in resurfacing of the same porcelain using coarse burs [7]. This edge damage may be attributed to stress concentration at bur/grit exits.

The relations between the maximum principal stresses and the dental operational parameters indicate that the maximum principal stresses were significantly dependent on both the feed rate and the depth of cut (ANOVA, $p<0.01$). As shown in Figure 4, the maximum principal stresses increased with feed rate. This is because that at a fixed depth of cut, an increase in feed rate does not result in a change in bur-prosthesis contact arc length but results in an increase in diamond grit depth of cut. An increase in diamond grit depth of cut could result in an increase in resurfacing force in the contact zone. Thus, the increasing force led to an increase to the maximum principal stress. Moreover, Figure 4 also shows that at any feed rate, smaller maximum principal stresses were obtained at the larger depth of cut. This is likely that this can be attributed to the fact that at a fixed feed rate, increasing the depth of cut resulted in both increases in diamond grit depth of cut and bur-prosthesis contact arc length.

Subsurface damage depths also exhibited significant dependence on the dental operational parameters (ANOVA, $p<0.01$). As shown in Figure 5, subsurface damage degrees showed upward trends with increase to either feed rate or depth of cut. This is consistent with studies on machining-induced damage in diamond grinding of engineering ceramics [19,20]. A previous study has reported that the average depths of subsurface damage induced in dental CAD/CAM machining of the same porcelain was 40–60 μm [19]. Our FEA prediction of subsurface damage depths are in the range 20–80 μm. Such subsurface damage could not only reduce the accuracy of fit of prostheses, but also lead to reduction in mechanical strength and lifetime of dental prostheses [21,22]. Therefore, in clinical practice, dental operational parameters should be carefully selected by considering both material removal rate and subsurface damage.

6 Conclusions

FEA modelling was conduced to simulate dental resurfacing of a feldspar porcelain. The results reveal that the maximum principal stresses induced by bur-prosthesis interactions were almost all concentrated at bur/grit exits. The maximum values of these stresses increased with the feed rate and decreased with the depth of cut. Increasing either the feed rate or the depth of cut resulted in an increase in subsurface damage depth. The results suggest that both the feed rate and the depth of cut are important parameters in controlling the degrees of subsurface damage in clinical dental resurfacing operations (ANOVA, $p<0.01$). This FEA modelling provides insights into the prediction of the quality of ceramic prostheses and guidance as to the proper selection of resurfacing operational parameters in dental practice.

Acknowledgements

This work was supported by the NSFC Project Grant No. 50475115. We thank Dr. Anthony Flynn of the Australian National University for valuable comments.

References

[1] Ironside JG, Swain MV. Ceramics in dental restorations–a review and critical issues. J Australasian Ceram Soc 1998; 34:78–91.

[2] Rosenblum M, Schulman A. A review of all-ceramic restorations. J Am Dent Assoc 1997; 128:297–307.

[3] Lawn BR, Deng Y, Thompson VP. Use of contact testing in the characterization and design of all-ceramic crownlike layer structures: a review. J Prosthet Dent 2001;86(5):495–510.

[4] Kelly JR. Clinically relevant approach to failure testing of all-ceramic restorations. J Prosthet Dent 1999; 81(6):652–661.

[5] Harvey CK, Kelly JR. Contact damage as a failure mode during in vitro testing. J Prosthodont 1996; 5:95–100.

[6] Rekow D, Thompson VP. Engineering long term clinical success of advanced ceramic prostheses. J Mater Sci: Mater Med 2007; 18: 47–56.

[7] Yin L, Jahanmir S, Ives LK. Abrasive machining of porcelain and zirconia with a dental handpiece. Wear 2003; 255: 975–989.

[8] Yin L, Song XF, Qu SF, Han YG, Wang H. Surface integrity and removal mechanism in simulated dental finishing of a feldspathic porcelain. J Biomed Mater Res B Appl Biomater 2006; 79B: 365–378.

[9] Zhang B, Peng XH. Grinding damage prediction for ceramics via CDM model. J Manufact Sci Eng 2000; 122: 51–58.

[10] Liu XB, Zhang B. Machining simulation for ceramics based on continuum damage mechanics. J Manufact Sci Eng 2002; 124: 553–561.

[11] Chuang T-J, Jahanmir S, Tang HC. Finite element simulation of straight plunge grinding for advanced ceramics. J Eur Ceram 2003; 23: 1723–1733.

[12] Subhash G, Zhang W. Finite element analysis of brittle cracking due single grit rotating scratch. J Appl Mech 2003; 70: 147–151.

[13] Yin L, Song XF, Qu SF, Huang T, Mei JP, Yang ZY, Li J. Performance evaluation of a dental handpiece in simulation of clinical finishing using a novel 2-DOF *in vitro* apparatus. Proc IME H J Eng Med 2006; 220:929–938.

[14] Deng Y, Lawn BR, Lloyd IK. Characterization of damage modes in dental ceramic bilayer structures. J Biomed Mater Res B Appl Biomater 2002; 63: 137–145.

[15] Kim H-W, Deng Y, Miranda P, Pajares A, Kim DK, Kim H-E, Lawn BR. Effect of flaw state on the strength of brittle coatings on soft substrates. J Am Ceram Soc 2001; 84: 2377–2384.

[16] Timoshenko SP, Goodier JN. Theory of elasticity. New York: McGraw-Hill Book Co; 1970.

[17] Malkin S. Grinding Technology: Theory and Applications of Machining with Abrasives. New York: Wiley; 1989.

[18] Hwang TW, Evans CJ, Malkin S. Size effect for specific energy in grinding of silicon nitride. Wear 1999; 225: 862–867.

[19] Maksoud TMA, Mokbel AA, Morgan JE. Evaluation of surface and sub-surface cracks of ground ceramic. Journal of Material Processing Technology 1999;88(1):222–243.

[20] Yui A, Watanabe T, Yoshida Y. Effect of grinding conditions upon bending strength of alumina ceramics. Grinding Fundamentals and Applications, ASME PED 1989;39:229–239.

[21] Sindel J, Petschelt A, Grellner F, Dierken C, Greil P. Evaluation of subsurface damage in CAD/CAM machined dental ceramics. J Mater Sci: Mater Med 1998; 9: 291–295.

[22] Shearer AC, Heymann HO, Wilson NH. Two ceramic materials compared for the production of CEREC inlays. J Dent 1993;21(5):302–304.